THE NATURE OF PHONONS AND SOLITARY WAVES IN α-HELICAL PROTEINS

ALBERT F. LAWRENCE,* JAMES C. MCDANIEL,‡ DAVID B. CHANG,‡ AND ROBERT R. BIRGE*
*Center for Molecular Electronics, Carnegie Mellon University, Pittsburgh, Pennsylvania 15213; and
‡Hughes Aircraft Company, Long Beach, California 90810

ABSTRACT A parametric study of the Davydov model of energy transduction in α-helical proteins is described. Previous investigations have shown that the Davydov model predicts that nonlinear interactions between phonons and amide-I excitations can stabilize the latter and produce a long-lived combined excitation (the so-called Davydov soliton), which propagates along the helix. The dynamics of this solitary wave are approximately those of solitons described using the nonlinear Schrödinger equation. The present study extends these previous investigations by analyzing the effect of helix length and nonlinear coupling efficiency on the phonon spectrum in short and medium length α-helical segments. The phonon energy accompanying amide-I excitation shows periodic variation in time with fluctuations that follow three different time scales. The phonon spectrum is highly dependent upon chain length but a majority of the energy remains localized in normal mode vibrations even in the long chain α-helices. Variation of the phonon–exciton coupling coefficient changes the amplitudes but not the frequencies of the phonon spectrum. The computed spectra contain frequencies ranging from 200 GHz to 6 THz, and as the chain length is increased, the long period oscillations increase in amplitude. The most important prediction of this study, however, is that the dynamics predicted by the numerical calculations have more in common with dynamics described by using the Frohlich polaron model than by using the Davydov soliton. Accordingly, the relevance of the Davydov soliton model was applied to energy transduction in α-helical proteins is questionable. We conclude that the Raman lines that have been assigned to solitons in *E. coli* are either associated with low frequency normal modes or are instrumental- or fluorescence-induced artifacts.

INTRODUCTION

A central issue in bioenergetics is how energy arising from chemical transformations is transferred across distances greater than 30 Å with high efficiency (Adey and Lawrence, 1984; Fröhlich, 1983; Davydov, 1982; Scott, 1981; Green, 1974). The amide-I (carbonyl stretching) vibration has been proposed as a possible vehicle for energy propagation in α-helical proteins (Green, 1974; Scott, 1981; Davydov, 1982; Fröhlich, 1983). Theoretical models based on this vehicle take two general forms: linear and nonlinear. Linear models of amide-I excitation predict decay to "thermal" vibrations within a few picoseconds. Both the timescale and the inefficiencies associated with thermalization of the excitation energy preclude use of the linear model to rationalize long distance energy transduction. These problems with the linear model prompted Davydov to propose a nonlinear model of energy transduction (Davydov, 1973, 1982). The "Davydov model," which is occasionally referred to as the "soliton model" because of its relationship to the nonlinear Schrödinger equation, has prompted considerable experimental (Webb, 1980, 1981; Del Giudice et al., 1982; Adey and Lawrence, 1984) and theoretical (Scott, 1982*a,b;* Drissler and Santo, 1983; Adey and Lawrence, 1984) interest. It would be a significant finding, indeed, to isolate a quantum-mechanical system whose dynamics were related to one of the soliton equations. An important consideration that had not attracted sufficient attention until recently (Lomdahl and Kerr, 1985; Lawrence et al., 1986) is the viability of the Davydov model under biologically relevant conditions. The present parametric study of this model for short and medium length α-helical protein is designed to test the viability of the Davydov model under boundary conditions designed to simulate inhomogeneities characteristic of biologically relevant environments.

THEORETICAL

Davydov's original model (Davydov, 1973; 1982) involves a chain of N molecules. The model is based on the assumption that transport of amide-I bond energy along a protein α-helix is, to a good approximation, the same as transport in a molecular crystal. Effects due to the interactions between hydrogen bonds, which stabilize the helix and covalent bonds, other than the amide-I, which constitute the protein backbone, are neglected. The Hamiltonian

Address offprint requests to Dr. Birge.

of the chain is written as the sum of exciton, phonon, and exciton–phonon interaction terms. We will review briefly the principal features of the single chain model.

The contribution due to nonperturbed excitons to the Hamilton of the chain may be written as a sum of the Hamiltonian for a system of noninteracting molecules and an interaction due to the Coloumb potential (Knox, 1963):

$$\mathcal{H}_{ex} = \sum_n H_n + \frac{1}{2}\sum_{n\neq m} V_{nm}, \tag{1}$$

where V_{nm} is the interaction between the nth and mth molecules of the chain. We assume that the molecules are constrained to two vibronic levels: a ground state, $|0\rangle$, and an excited state, $|f\rangle$. Furthermore, if ϕ_n^1 represents the excited state wavefunction and ϕ_n^0 the ground state, then the wavefunction Φ^I of the chain may be written as a linear combination of the functions

$$\Phi^I = \phi_1^{i_1}\,\phi_2^{i_2}\ldots\phi_N^{i_N}, \tag{2}$$

where i_n is either 0 or 1. This representation gives rise to the usual definitions of occupation number, number operator, and annihilation and creation operators in the second quantization. In particular, the nth occupation number N_{nf} of Φ^I is 1 if $i_n = 1$, and 0 otherwise. Furthermore,

$$N_{nf}\Phi^I = N_{nf} \tag{3a}$$

$$b_{nf}^{+}\Phi^I = (1 - N_{nf})\,\Phi^{I'}, \quad I' = (i_1, \ldots, i_n + 1, \ldots, I_N) \tag{3b}$$

$$b_{nf}\Phi^I = N_{nf}\Phi^{I''}, \quad I'' = (i_1, \ldots, i_n - 1, \ldots, i_N). \tag{3c}$$

Note that $b_{n0}^{+} = b_{nf}$ in a two-level model. These operators satisfy the Pauli commutation relations:

$$b_{nf}\,b_{nf}^{+} = b_{nf}^{+}\,b_{nf} = 1 \tag{4a}$$

$$b_{nf}\,b_{mf} = b_{mf}\,b_{nf}, \quad n \neq m \tag{4b}$$

$$b_{nf}^{+}\,b_{mf} = b_{mf}\,b_{nf}^{+}, \quad n \neq m. \tag{4c}$$

The Hamiltonian (Eq. 1) may be written in the occupation number representation as follows:

$$\mathcal{H}_{ex} = \Sigma\,\epsilon_f\,b_{nf}^{+}\,b_{nf} = (1/2)\,\Sigma\,b_{nf'}^{+}\,b_{mg'}^{+}\,b_{mg}b_{nf}\,\langle f'g'|V_{nm}|gf\rangle \tag{5}$$

where ϵ_f is the energy of excitation of an isolated molecule and the second summation is over m and n representing different sites, or f and g representing different states if the sites m and n are the same.

If we write

$$B_n = b_{n0}^{+}\,b_{nf}, \quad B_{nf}^{+} = b_{nf}^{+}\,b_{n0},$$

then the operator B_n changes the excited state to the ground state and the operator B_n^{+} changes the ground state to the excited state at site n. If we neglect all but the nearest neighbor interactions and further restrict the terms arising from Eq. 1 to those given by the Heitler–London approximation, the Hamiltonian (Eq. 5) may be written as follows:

$$\mathcal{H}_{ex} = \Delta\sum_n B_n^{+}B_n - J\sum_n (B_{n+1}^{+}B_n + B_n^{+}B_{n+1}). \tag{6}$$

In this formula Δ is the molecular excitation energy, and J is the energy of resonant interaction of neighboring molecules. Note that annihilation operators of the exciton model, as presented, satisfy Bose statistics (Knox, 1963). Further details relating to the derivation of Eqs. 5 and 6 may be found in Davydov (1971).

We turn now to the phonon terms. The treatment follows the standard model of a linear chain of harmonic oscillators (Knox, 1963; Haken, 1976). The phonon Hamiltonian has the form:

$$\mathcal{H}_{ph} = \frac{1}{2}M\sum_n p_n^2 + \omega/2\sum_n (u_n - u_{n-1})^2, \tag{7}$$

where p_n is the momentum conjugate to the displacement u_n, ω is the elastic coupling constant of the chain, and M is the molecular mass. The dispersion relation for phonons in an infinite chain is given by:

$$\Omega_q = 2(V_\alpha/R_0)|\sin(qR_0/2)|, \tag{8}$$

where q is the wave vector, V_α is the velocity of sound, and Ω_q is the angular frequency. In the second quantization, p_n and u_n are replaced by operators $\hat{\mathbf{P}}_n$ and $\hat{\mathbf{U}}_n$. The momentum and displacement operators satisfy the canonical communication relation:

$$[\hat{\mathbf{U}}_m, \hat{\mathbf{P}}_n] = i\hbar\delta_{nm}. \tag{9}$$

The final contribution to the Hamiltonian in the Davydov model is the interaction term. The interaction of excitons with phonons is given by:

$$\mathcal{H}_{int} = \chi\,\Sigma\,B_n^{+}B_n(\hat{\mathbf{U}}_{n+1} - \hat{\mathbf{U}}_{n-1}), \tag{10}$$

where χ is the exciton–phonon coupling parameter. This term can be considered as a change in amide-I bond energy due to stretching or compression of the helix. The total Hamiltonian for the chain is written as:

$$\mathcal{H}_{sol} = \mathcal{H}_{ex} + \mathcal{H}_{ph} + \mathcal{H}_{int}. \tag{11}$$

A particular solution for the time-dependent Schrödinger equation associated with ψ_s is given by the following wavefunction:

$$|\psi_s(t)\rangle = \sum_n [C_n(t)\exp\sigma(t)\,B_n^{+}|0\rangle], \tag{12}$$

where $C_n(t)$ is the probability amplitude of an exciton occupying site n at time t, and the term $\exp\sigma(t)$ arises from a coherent state representation of the phonons (Louisell, 1973). This wavefunction is termed the "Davydov ansatz" (Venzl and Fischer, 1985). In particular, the operator $\sigma(t)$ is defined as follows:

$$\sigma(t) = i/\hbar\sum_j [\beta_j(t)\hat{\mathbf{P}}_j - \pi_j(t)\hat{\mathbf{U}}_j]. \tag{13}$$

Eq. 12 gives the wavefunction ψ_s as a product of phonon and exciton wavefunctions. Conservation of number implies the normalization condition:

$$\Sigma|C_n(t)|^2 = 1. \tag{14}$$

Note that $C_n(t)$, $\beta_n(t)$, and $\pi_n(t)$ are functions to be determined. Both β_n and π_n may be interpreted in terms of the coherent state representation (see Haken, 1976).

Explicit expressions for the functions $\beta_n(t)$, $\pi_n(t)$, and $C_n(t)$ can be derived via the time-dependent Schrödinger equations. A specific derivation may be found in Lomdahl and Kerr (1985).

The equations for a single chain may be generalized to

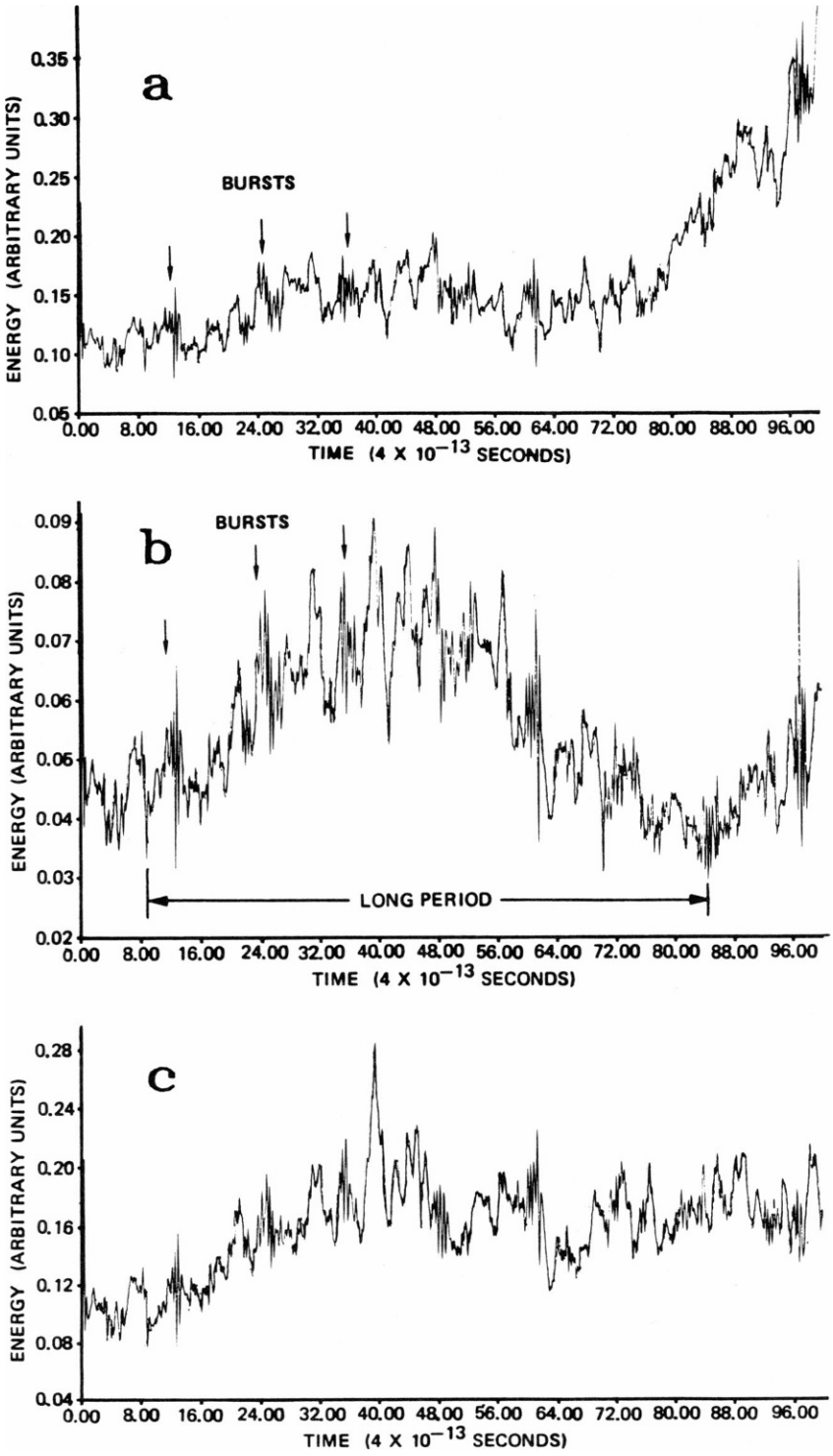

FIGURE 1 The total phonon energy of a 27-residue α-helix plotted as a function of time (1 unit = 0.4 ps) for coupling coefficients of 0.2×10^{-10} Newtons (*a*), 0.4×10^{-10} Newtons (*b*), and 0.6×10^{-10} Newtons (*c*). Bursts of ~6 THz oscillations are observed at time intervals of ~4.8 ps (examples are indicated with arrows). A long-period fluctuation is clearly evident in the phonon spectrum in *b*.

the case of three interacting chains required to describe a protein α-helix. In this model, resonance interactions may occur along the protein helix. Adding these interactions to the model yields a system of coupled equations in which the dynamic variables are indexed by spine number as well as position along each hydrogen-bonded spine. Details may be found in Scott (1982*a*,*b*).

Our calculations are based on a coupled system of ordinary differential equations, obtained as outlined in the previous section. Except for choice of boundary conditions, our procedures are formally equivalent to those of Hyman et al. (1981). The salient difference is that the ends of the helix are not spatially constrained. The complete model is given by the following system of equations in which i represents the spine number, and n the position along the spine. We are representing exciton amplitudes by $C_{n,i}$, the phonon coherent state amplitudes by $\beta_{n,i}$.

$$\begin{aligned}\frac{i\mathrm{d}C_{n,i}}{\mathrm{d}t'} = {} & (1.41)C_{n,i}\sum_n [(\mathrm{d}\beta_{n,i}/\mathrm{d}t')^2 + (\beta_{n+1,i} - \beta_{n,i})^2] \\ & -0.058(C_{n-1,i} + C_{n+1,i}) \\ & + 0.092(C_{n,i+1} + C_{n,i-1}) \\ & + 0.372(10^{10}\chi)\,[(1 - \delta_N^n)(\beta_{n+1,i} - \beta_{n,i})C_{n,i} \\ & + (1 - \delta_0^n)(\beta_{n,i} - \beta_{n-1,i})C_{n,i} \\ & + (1 - \delta_N^n)C_{n+1,i}\,(\beta_{n+1,i} - \beta_{n,i}) \\ & + (1 - \delta_0^n)C_{n-1,i}(\beta_{n,i} - \beta_{n-1,i})]. \qquad (15a)\end{aligned}$$

$$\begin{aligned}\frac{\mathrm{d}\beta_{n,i}}{(\mathrm{d}t')^2} = {} & (1 - \delta_N^n)(-\beta_{n+1,i} + \beta_{n,i}) \\ & + (1 - \delta_0^n)(\beta_{n,i} - \beta_{n-1,i}) + 0.132(10^{10}\chi) \\ & \times \{(1 - \delta_N^n)(1 - \delta_0^n)[|C_{n+1,i}|^2 - |C_{n-1,i}|^2] \\ & + \delta_0^n[|C_{n,i}|^2 + |C_{n-1,i}|^2] \\ & - \delta_N^n[|C_{n-1,i}|^2 + |C_{n,i}|^2] \\ & + C_{n+1,i}^*(C_{n+1,i} - C_{n-1,i}) \\ & + (C_{n+1,i}^* - C_{n-1,i}^+)C_{n,i}\}, \qquad (15b)\end{aligned}$$

where $\delta_j^i = 0$ unless $i = j$ and $N \geq 2$. Use of δ_j^i in these formulas gives the boundary conditions, which arise from the free boundary assumptions, and modification of the Hamiltonian H_{sol} to account for end conditions. The numerical coefficients are as in Hyman et al. (1981) and may be derived from known parameters for protein molecules. The exciton–phonon coupling coefficient remains the only adjustable parameter in this model.

RESULTS

Unless stated otherwise, calculations were started with a single excitation in the first bond ($C_{0,1}(0) = 1$) and no phonon states populated ($\beta_{n,i}(0) = 0$ for all n, i). The total phonon energies as a function of time for a chain length of 27 residues are displayed in Fig. 1. Over thirty plots of phonon energy versus time for various cases were examined. In every case the initial transients in phonon energy levels were very short compared with total time intervals. Analysis of phonon–exciton coupling is enhanced by examining the modulus of the Fourier transform of the total phonon energy, which yields the power spectrum as a function of frequency (Fig. 2). Power spectra as a function of chain length and nonlinear coupling coefficiency are shown in Figs. 3 and 4. Examination of Fig. 1 indicates that several different oscillatory time scales are present, indicative of different phonon–exciton energy exchange processes.

Short period fluctuations (4–6 THz) appear in transient bursts that recur at periodic intervals. These intervals are separated by time spans that are roughly proportional to the chain length (~3.2 ps for a chain length of 18, ~4.8 ps for a chain length of 27 [Fig. 1]). Although the durations of the bursts appear to be independent of chain length, the proportion of energy fluctuations at lower frequencies increase rapidly with chain length. Furthermore, only for the 18-residue case were the 5.5-THz fluctuations observed to constitute a significant portion of the fluctuations spectrum. We suggest that these fluctuations repre-

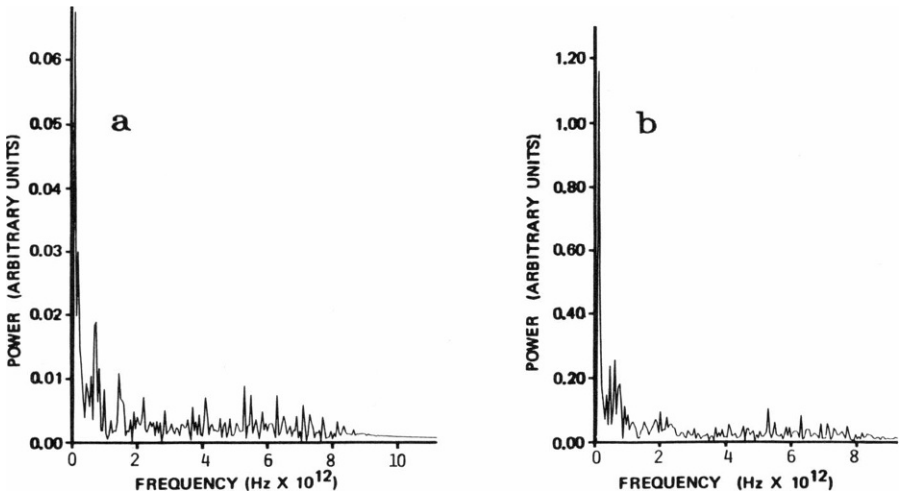

FIGURE 2 Fourier transforms of the total phonon energy for α-helices of 27 residues (*a* and *b*). The calculations were carried out using coupling coefficients of 0.2×10^{-10} Newtons (*a*) and 0.6×10^{-10} Newtons (*b*).

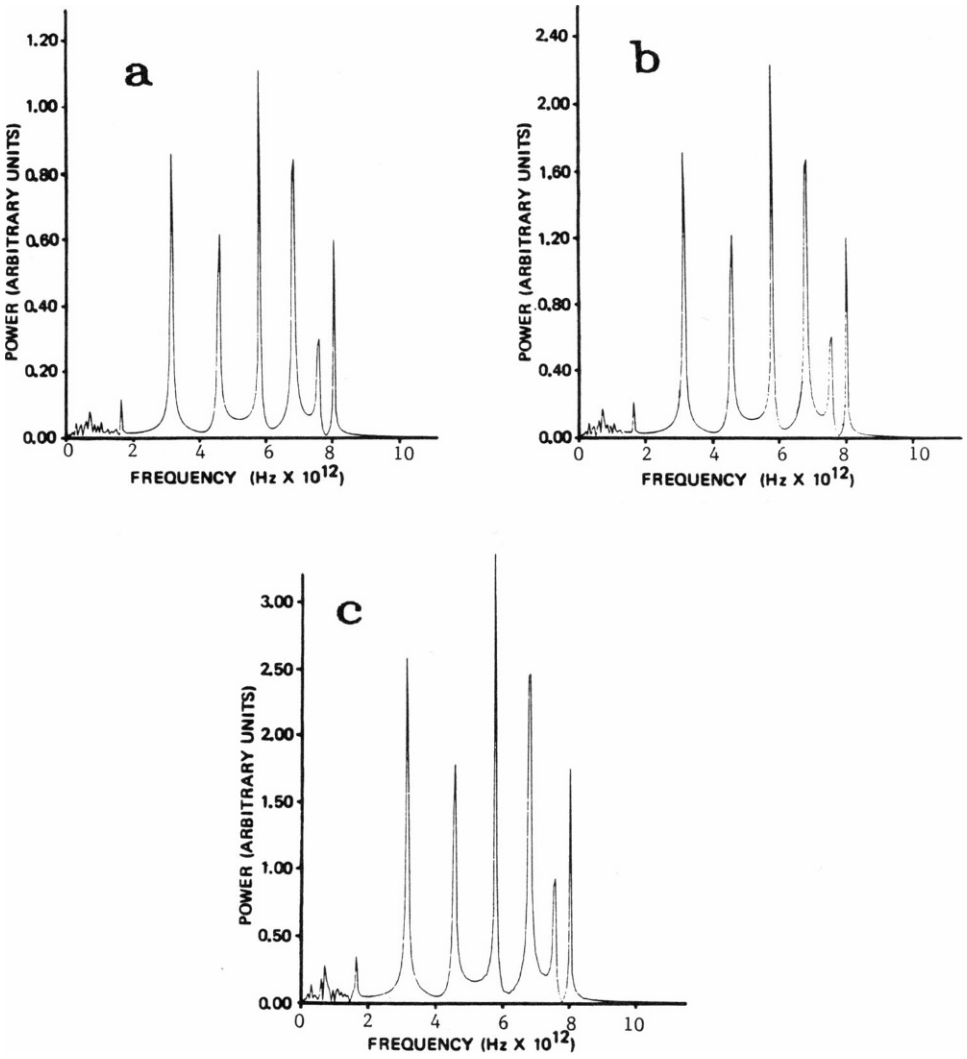

FIGURE 3 Phonon spectra obtained by taking the Fourier transforms of momenta for intramolecular dynamics in the center of an α-helix of 24 residues for coupling coefficients of 0.2×10^{-10} Newtons (a), 0.4×10^{-10} Newtons (b), and 0.6×10^{-10} Newtons (c). Note that the relative amplitudes and frequencies of the resonances are independent of coupling coefficient.

sent an accidental resonance between exciton and phonon modes because a peak at precisely the fluctuation frequency also appeared in the phonon spectra plots for 18 residues (Fig. 2).

Intermediate period fluctuations (500 GHz–1 THz) are observed, which are proportional to the chain length. These fluctuations occur on a shorter time period than the burst repeat intervals (200–500 GHz), and decrease in power amplitude as chain length increases.

Long period fluctuations (~100 GHz) are observed for residue numbers larger than 23 and in several cases were followed for many periods (not shown). The amplitude of these fluctuations shows a pronounced dependence on both chain length and nonlinear coupling efficiency with a maximum amplitude appearing for a chain length of 27 residues and a coupling coefficient of 0.4×10^{-10} Newtons (Fig. 1).

Although analysis of the above phonon–exciton interaction provides insight into energy transduction processes along the α-helix, phonon energy is not subject to direct experimental observation. Accordingly, we also calculated the momentum expectation value, $\beta(t)$, for selected residues along the chain. The modulus of the Fourier transform of $\beta(t)$ yields the phonon spectrum, as can be seen from inspection of Eq. 9 and the relation $\beta_n(t) = \langle \psi_s(t) | \hat{U}_n | \psi_s(t) \rangle$. To analyze the collective modes, we evaluated the sum of momenta for residues 1, 2, and 3 (the three end residues) and the sum of momenta for residues $[n/2]$, $[n/2] - 1$, and $[n/2] - 2$. We also calculated the modulus of the Fourier transform of each momentum plot. Plots of amplitude versus frequency are shown in Figs. 3 and 4. Each of the latter plots consists of a series of discrete maxima, with each peak corresponding to a normal mode of the protein chain and following the sin ($q R_{0/2}$) form for the dispersion relation given in Eq. 8. In particular, the ℓ-th mode of a harmonic lattice with free ends is given by

$$y_n = \frac{2}{N} a_k \sin\left[2\left(\frac{\omega}{M}\right)^{1/2} \sin\left(\frac{k}{2}\right)t\right] \cos\left[(2n-1)k\right], \quad (16a)$$

where

$$k = \frac{\pi \ell}{N} \qquad 0 \le \ell \le N-1, \quad (16b)$$

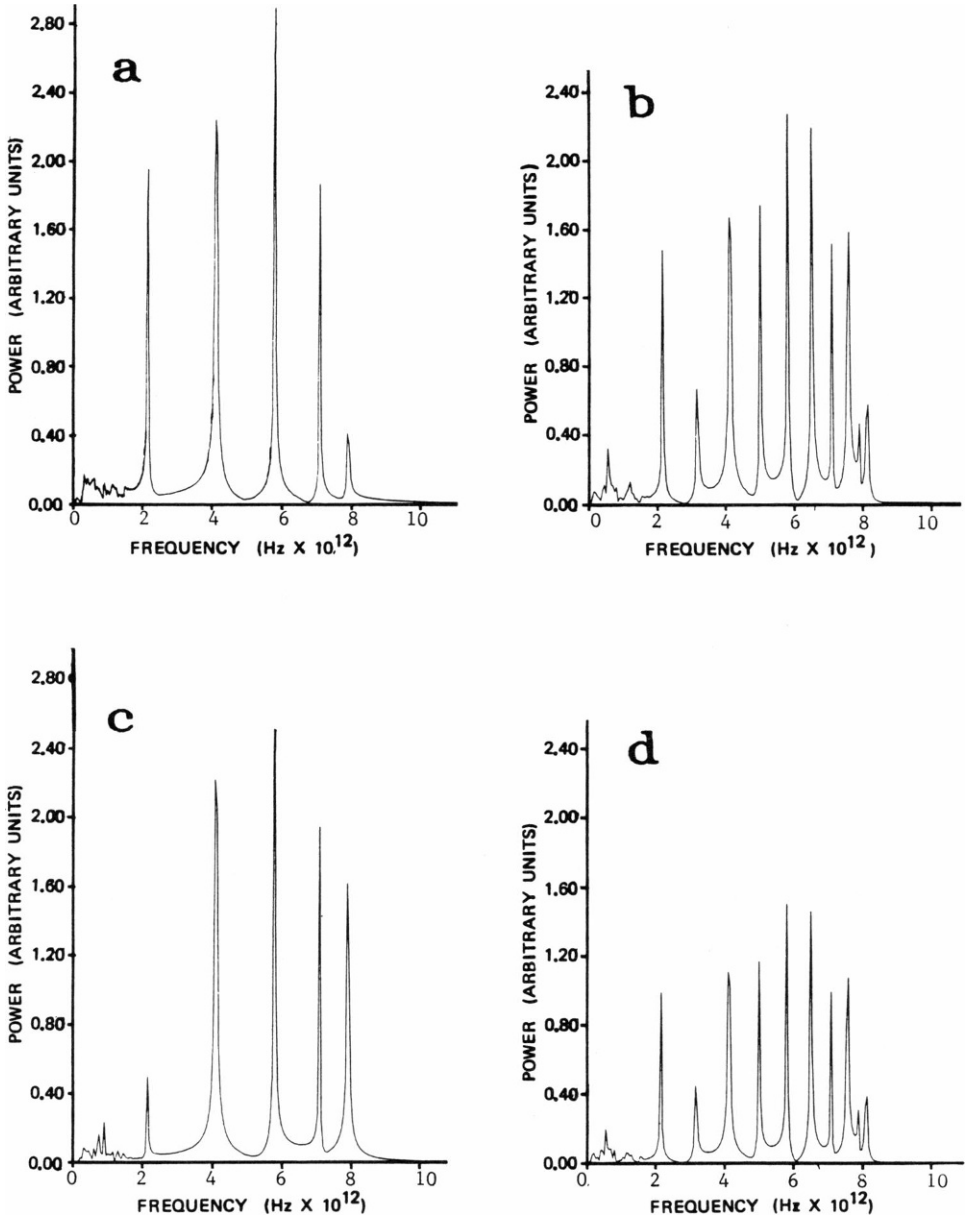

FIGURE 4 Phonon spectra obtained by taking the Fourier transforms of momenta for intramolecular dynamics within α-helices of 18 and 36 residues: (*a*) 18 residues, center of chain; (*b*) 36 residues, center of chain; (*c*) 18 residues, end of chain; and (*d*) 36 residues, end of chain. The calculations were carried out using a nonlinear coefficient of 0.4×10^{-10} Newtons. Note that the number of primary resonances double in going from the shorter to the longer α-helix and that the frequencies of the phonon modes in the shorter chain are observed in the longer chain.

and y_n denotes the displacement of the nth mass, and N is the number of masses in the chain (Haken, 1976; Jackson, 1978). This gives frequencies of

$$\frac{\left(\frac{\omega}{M}\right)^{1/2} \sin\left(\frac{\pi \ell}{2N}\right)}{\pi} \quad \text{for } \ell = 0, \ldots, N-1.$$

The values used in our computations give, as in Hyman et al., a fundamental frequency

$$\left(\frac{\omega}{M}\right)^{1/2} / \pi = 8.1 \times 10^{12} \text{ Hz}.$$

This may be observed as a band edge on our phonon spectra.

DISCUSSION

Interpretation of the results reported above is best accomplished by evaluating simplified versions of Eqs. 15a and 15b, which are generated by neglecting all coupling terms of negligible to small relative magnitude:

$$\frac{i\mathrm{d}C_{n,i}}{\mathrm{d}t'} = 0.372(10^{10}\chi)[(\beta_{n+1,i} - \beta_{n,i})C_{n,i} + (\beta_{n,i} - \beta_{n-1,i})C_{n-1,i}] - 0.058(C_{n+1,i} + C_{n-1,i}) + 0.092(C_{n,i+1} + C_{n,i-1}). \quad (17a)$$

$$\frac{\mathrm{d}^2\beta_{n,i}}{\mathrm{d}t'^2} = 2\beta_{n,i} - \beta_{n+1,i} - \beta_{n-1,i} + 0.132(10^{10}\chi)[|C_{n+1,i}|^2 + |C_{n-1,i}|^2]. \quad (17b)$$

In particular, Eq. 17a assumes that the energy of the amide-I carbonyl bond is a function of only one external influence, namely the strength of the hydrogen bond on the carbonyl side of the peptide unit. Excitons are therefore described by a system of linear autonomous equations:

$$\frac{i\mathrm{d}\mathbf{C}}{\mathrm{d}t} = K\mathbf{C}, \tag{18}$$

where K is a linear operator and $\mathbf{C}$ is a state vector describing exciton distribution along the chain. If we assume the phonons are fixed this equation has a solution of the form $\mathbf{A} = \exp(iKt)\mathbf{A}_0$. Similarly, phonon displacement is described by the approximation:

$$\frac{i\mathrm{d}B}{\mathrm{d}t'} = LB + F, \tag{19}$$

where $B_{n,i}$ is given by $(\beta_{n,i}, \beta_{n,i})$, L is a linear operator, and F is the nonlinear term defined by solution of the above exciton equation. A closed form solution of Eq. 19 may be made on assuming a fixed exciton distribution:

$$B(t) = \int_0^t \exp[iL(t-\tau)]F(\tau)\mathrm{d}f\tau + \exp(iLt)B. \tag{20}$$

By iterating the solution process at small time steps we may obtain a self-consistent evaluation of the above equations. Examinations of Eq. 19 for χ in the range 0.2×10^{-10}–0.6×10^{-10} neutrons indicates that the average lifetime of an exciton at a single peptide unit is ~1.6 ps (see Fig. 5). The lifetime of a "localized" exciton is sufficiently long to overlap with the manifold of phonon states, and the occurrence of exciton–phonon resonances is therefore responsible for the transient bursts that characterize the

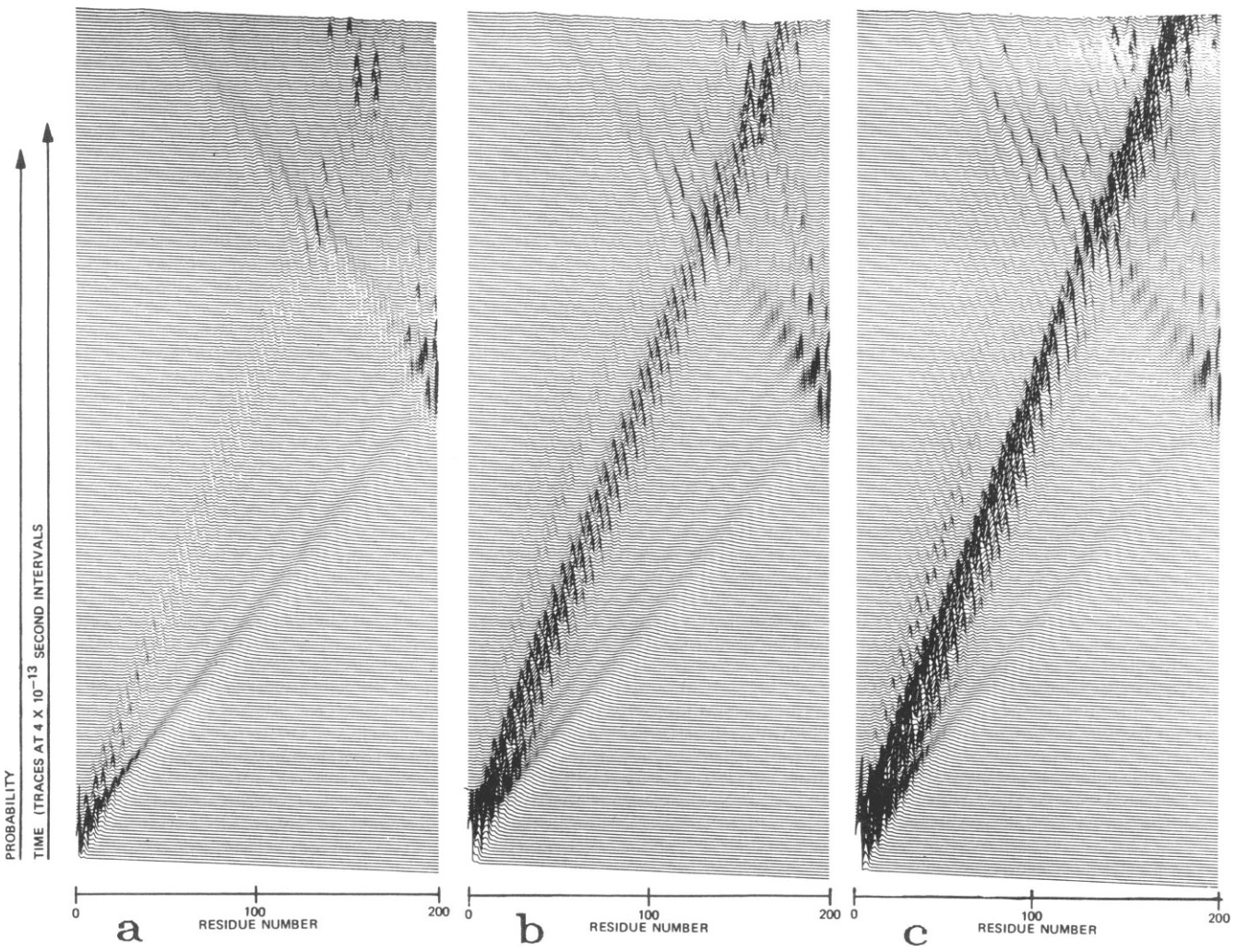

FIGURE 5 Probability of exciton occupation as a function of residue (horizontal axis) and time (each trace represents a time increment of 0.4 ps with time increasing in going from the bottom to the top of the figure). The calculations were carried out for a nonlinear coefficient of 0.5×10^{-10} Newtons for different initial quanta of excitation of the amide-I carbonyl vibration: one quanta (*a*), two quanta (*b*), and three quanta (*c*). Note that three modes of propagation are seen to emerge for the three-quanta case and may correspond to a superposition of states. The progression of figures illustrate the progressive increase of the probability for soliton formation from <0.1 for one quantum to ~0.7 for three quanta. These estimates may be obtained by a restating of the normalization condition given in Eq. 14 to be $\Sigma_n|C_n(t)^2| = N$, where N is the number of excitons.

short fluctuations observed in the phonon energy spectrum. Because exciton–phonon coupling is strongest when the probability of an exciton occupying an end-group is highest, periods between bursts correspond to the periods between occupation of the end residues by excitons. The origin and reappearance rate of the transient bursts is therefore a consequence of a time dependence of the exciton–phonon coupling. Note that Eq. 17 may also be easily extended to give a phenomenological treatment of the thermalized case by adding a random force to the F term (Kubo, 1957). A more complete treatment of the long-chain case under thermal conditions may be found in Lawrence et al. (1986). This treatment may be generalized to a Fokker–Planck equation for the phonon displacements by adding a noise term to Eq. 17b and applying the techniques described by Risken (1985).

Evaluation of the simplified equations suggests that the medium period oscillations are due to resonances between phonons and the periodicity of the excitons. This analysis is based largely on the observation that the amplitude and frequency of these fluctuations are linearly related to chain length.

Finally, the long frequency fluctuations of the phonon energy represent the precursors to the solitons that are theoretically predicted to exist in very long chain (>200 amino acid residues), homogeneous α-helices. It is important to note, however, that these oscillations are much closer in formal description to a normal mode of the α-helix than to a stationary wave (or soliton). The low cross-section for a soliton to form from a single excitation casts doubt on the validity of the continuum approximation, which was originally used to predict a solitonic solution of the dynamical equations (Davydov, 1973).[1] Fig. 5 indicates a superposition of states between the dispersive mode and the nondispersive, solitonic mode of exciton propagation. For the one-quantum case the probability of soliton formation is <0.1. As indicated by the first part of this figure and previously argued by Scott that direct radiative transfer is forbidden on the basis of Franck–Condon factors (Scott, 1984), at least two excitons must be placed in adjacent sites before there is a significant probability a soliton will form. A proper formulation for a two-exciton state would include at least fourth-order terms in the exciton Hamiltonian such as $\Sigma I_{m'n'mn} P_{m'}^{+} P_{n'}^{+} P_m P_n$, where I gives the interaction strength (Satarić et al., 1981). The dynamical equations arising from this extended Hamiltonian do not have the same continuum approximation as the Davydov Hamiltonian. Therefore, it is necessary to show that higher order effects in the exciton system and the exciton–phonon coupling are negligible. In the absence of further numerical analysis, our calculations suggest that the unique physical characteristics that permit soliton formation are a long homogeneous (α-helical) chain and a rather delicate relation between nonlinearities due to phonon–exciton and nonlinearities due to exciton–exciton interactions. This is borne out by the parametric studies of Lawrence et al. (1986), which show that for physiological temperatures, thermal vibrations inhibit soliton formation for a wide range of values of the coupling parameter. Accordingly, the formation of Davydov solitons in vivo is unlikely due to the above constraints, which cannot be accommodated in biological environments due to inhomogeneous intramolecular and intermolecular forces. The Raman lines (Webb and Dodds, 1968; Webb and Booth, 1969; Webb 1980, 1981) that have been assigned to the Davydov soliton in proteins in living cells (Lomdahl et al., 1982) are more likely to be normal modes, instrumental artifacts, or vibronic bands associated with fluorescent impurities. The latter was recently proposed as a viable possibility on the basis of experimental studies by Layne et al. (1985). These researchers observed transient fluorescence in synchronously dividing *E. coli*.

Because normal-mode dynamics persist in the Davydov model applied to polypeptide chains at low temperatures, we believe that a further look at the fundamental model is in order. The small polaron Hamilton (Mahan, 1981) has been proposed (Lomdahl and Kerr, 1986; Brown et al., 1986) as a basis for an appropriate generalization. In particular, the H_{int} term of H_{sol} (Eq. 11) is replaced by

$$H_{int} = \sum_{q,m} \chi_m^q \, \hbar\omega_q \, (b_q^{+} + b_{-q}) \; B_m^{+} B_m^{+}. \qquad (21)$$

Here, the sum is over all the normal modes of the molecule and sites of amide-I excitation. Small polaron dynamics are actually observed in numerical simulations as the exciton–phonon coupling is increased (Lawrence et al., 1986). An assessment of the gain in realism achieved by including more vibrational modes in the Hamiltonian awaits further experimental studies on the spectra of hydrogen-bonded amide systems.

It should also be noted that there is some disagreement in the literature concerning the correct form of the Davydov ansatz. Brown et al. (1986) claim to have shown that the wavefunction given by Eqs. 12 and 13 cannot represent a single polaron state. This latter state is the wavefunction arising from Eqs. 6 and 11 with J set equal to 0. Lomdahl et al. claim that equations of motion based on the ansatz of Eq. 12 may be derived by substitution of the wavefunction into the Schrödinger equation. Although both may be correct, because different Hamiltonians are used for the

[1]Proper quantum-mechanical treatment of an integrable nonlinear field equation requires an infinite system of eigenstates, as given by the Bethe ansatz (Thacker, H.B., 1981, *Rev. Mod. Phys.*, 53:253) or requires carrying a nonlinear potential in a lattice approximation (Gallavotti, G., 1985, *Rev. Mod. Phys.*, 57:471). A naive application of the continuum approximation to the dynamical equations of a molecular system ignores the problem of consistency with the spatial derivatives in the underlying Hamiltonian operator. Furthermore, the emergence of quantum-mechanical effects such superposition of states in calculations based on the Davydov model shows that some care must be exercised in relating dynamically stable propagation of excitons to the classical solutions of the nonlinear Schrödinger equation.

chain, the ansatz of Eq. 12 represents a linearization of the coupling between excitons and phonons. The Hamiltonian given by Eqs. 6, 7, and 21 substituted into Eq. 11 yields

$$\sigma(t) = i/\hbar \Sigma [\beta_{nq}(t)b_q^+ + \beta^* nq(t)b_q] \qquad (22)$$

in Eq. 12. A more complete theory of coherent phonon states in molecular systems would have some interesting consequences. The first consequence would be a rigorous justification of semiclassical treatments of molecular dynamics. This is because coherent phonon states are states of minimal uncertainty, and thus constitute the quantum states most amenable to classical approximation. The second, more technical advantage of a coherent state treatment is that such states can be represented as orbits of a unitary group on states of a quantum dynamical system (D'Ariano and Rosetti, 1985). In particular, this observation makes possible the application of Lie algebra theory to the simulation of molecular dynamics. This application is currently under investigation.

This work was supported in part by grants from the National Institutes of Health (GM-34548) and the Office of Naval Research (N1483-C-100).

Received for publication 25 August 1986 and in final form 12 January 1987.

REFERENCES

Adey, W. R., and A. F. Lawrence. 1984. Nonlinear Electrodynamics in Biological Systems. Plenum Publishing Corp., New York.

Brown, D. W., B. J. West, and K. Lindenberg. 1986. Davydov solitons: new results at variance and standard derivations. *Phys. Rev.* A33:4110.

D'Ariano, G. M., and M. G. Rosetti. 1985. Soliton equations, τ-functions and coherent states in integrable systems in statistical mechanics. G. M. D'Ariano, A. Montorsi, and M. G. Rosetti, editors. World Scientific Publishing Co., Singapore. 143–152.

Davydov, A. S. 1971. Theory of Molecular Excitons. Plenum Publishing Corp., New York. 113–124.

Davydov, A. S. 1973. The theory of contraction of proteins under their excitation. *J. Theor. Biol.* 38:559–569.

Davydov, A. S. 1982. Biology and Quantum Mechanics. Pergammon Press, Oxford. 185–212.

Del Giudice, E., S. Doglia, and M. Milani. 1982. A collective dynamics in metabolically active cells. *Physica Scripta.* 26:232–238.

Drissler, F., and L. Santo. 1983. Coherent excitations and the Raman effect. *In* Coherent Excitations in Biological Systems. H. Fröhlich and F. Kremer, editors. Springer-Verlag GmbH & Co., Heidelberg, Berlin. 6–9.

Frölich, H. 1983. Coherence in biology. *In* Coherent Excitations in Biological Systems. H. Fröhlich and F. Kremer, editors. Springer-Verlag GmbH & Co., Heidelberg, Berlin. 1–5.

Green, D. E. 1974. A framework of principles for the unification of bioenergetics. *Ann. NY Acad. Sci.* 227:6–27.

Haken, H. 1976. Quantum Field Theory of Solids. Elsevier North-Holland, New York. 49–60.

Hyman, J. M., D. W. McLaughlin, and A. C. Scott. 1981. On Davydovs alpha-helix solitons. *Physica.* 3D:23–44.

Jackson, E. A. 1978. Nonlinearity and irreversibility in lattice dynamics. *Rocky Mt. J. Math.* 8:127.

Knox, R. S. 1963. Theory of Excitons. Academic Press, Inc., New York. 1–6, 87–101, 136–163.

Kubo, R. 1957. Statistical-mechanical theory of irreversible processes. I. General theory and simple applications to magnetic and conduction problems. *J. Phys. Soc. Japan.* 12:570.

Lawrence, A. F., J. C. McDaniel, D. B. Chang, B. M. Pierce, and R. R. Birge. 1986. Dynamics of the Davydov model in α-helical proteins: effects of coupling parameter and temperature. *Phys. Rev. A.* 33:1188.

Layne, S. P., I. J. Bigio, A. C. Scott, and P. S. Lomdahl. 1985. Transient fluorescence in synchronously dividing *Escherichia Coli. Proc. Natl. Acad. Sci. USA.* 82:7599.

Lomdahl, P. S., L. MacNeil, A. C. Scott, M. E. Stoneham, and S. J. Webb. 1982. An assignment to internal soliton vibrations of laser-Raman lives from living cells. *Phys. Lett.* 92A:207–210.

Lomdahl, P., and W. C. Kerr. 1985. Do Davydov solitons exist at 300 K? *Phys. Rev. Lett.* 55:1235.

Lomdahl, P., and W. C. Kerr. 1986. Finite Temperature Effect on Models of Hydrogen-bonded Polypeptides. Los Alamos National Laboratories, Los Alamos, NM. LA-UR-86-499.

Louisell, W. H. 1973. Quantum Statistical Properties of Radiation. John Wiley & Sons, Inc., New York. 104–109.

Mahan, G. D. 1981. Many-Particle Physics. Plenum Publishing Corp., New York.

Risken, H. 1985. The Fokker-Planck Equation. Springer Valley, New York.

Satarić, M. G. Vujičić, and R. Zakula. 1981. Biexcitons as solitons in the one-dimensional molecular crystal. *Il. Nuovo. Cimento.* 63:709–723.

Scott, A. C. 1981. The laser-Raman spectrum of Davydov soliton. *Phys. Lett.* 86A:60–62.

Scott, A. C. 1982*a*. Dynamics of Davydov soliton. *Phys. Rev. A.* 26:578–595; Erratum: Dynamics of Davydov solitons. 27:2767.

Scott, A. C. 1982*b*. The Vibrational structure of Davydov solitons. *Physica Scripta.* 25:651–658.

Scott, A. C. 1984. Solitons and bioenergetics. *In* Nonlinear Electrodynamics in Biological Systems. W. R. Adey and A. F. Lawrence, editors. Plenum Publishing Corp., New York.

Venzl, G., and S. F. Fischer. 1985. Theory of exciton-phonon coupling in one-dimensional molecular crystals: a variational treatment with delocalized solitary states. *Phys. Rev. B.* 32:6437.

Webb, S. J. 1980. Laser-Raman spectroscopy of living cells. *Phys. Rep.* 60:201–224.

Webb, S. J. 1981. Techniques for the study of living cells by resonance and microwave spectroscopy. *Collect. Phenom. (Lond.).* 3:313–320.

Webb, S. J., and D. D. Dodds. 1968. Inhibition of bacterial growth by 136gc microwaves. *Nature (Lond.).* 218:374–375.

Webb, S. J., and A. D. Booth. 1969. Absorption of microwaves by microorganisms. *Nature (Lond.).* 222:1199–1200.